TWMS J. App. and Eng. Math. V.15, N.4, 2025, pp. 982-993

TRANSITION TO CHAOS IN HIGH CONTROL PARAMETER OF SWIFT–HOHENBERG EQUATION

F. NUGROHO[1*], H. N. WIJAYA[2], §

ABSTRACT. The Swift-Hohenberg equation, which is a parabolic equation, is studied at high values of the control parameter. The method used is exponential time differencing combined with fourth-order Runge-Kutta (ETDRK4). The solution obtained was subjected to spectral analysis. In the case of real equations, it can be shown that there is a transition from regular to chaotic dynamics at the control parameter of 23.6. Meanwhile, in the case of equations with complex terms, transition to chaotic dynamics occurs at low control parameter and the imaginary constant range of $-8 \leq b \leq -6$. It can be concluded that the Swift-Hohenberg equation can produce chaotic dynamics at certain parameter values.

Keywords: Swift-Hohenberg equation, ETDRK4, dynamic transition, chaotic dynamics.

AMS Subject Classification: 35G20, 37M05

1. INTRODUCTION

The Swift-Hohenberg equation is a fourth-order nonlinear partial differential equation that describes the spatiotemporal evolution of a perturbation field [1]. This equation can be used as a model for pattern formation in the Rayleigh-Bénard convection system caused by convective instability. Its one-dimensional version is

$$\partial_t u = (\epsilon - 1 - 2\partial_x^2 - \partial_x^4)u - u^3, \tag{1}$$

where $u(x,t)$ is a function of position x and time t, and ϵ is a control parameter that corresponds to the driving parameter in the Rayleigh-Bénard system, represented by the temperature difference ΔT that drives the system away from equilibrium [2]. The above equation can be written as a sum of linear and nonlinear terms:

$$\partial_t u = \mathcal{L}u - N[u], \tag{2}$$

[1] Department of Physics, Faculty of Mathematics and Natural Sciences, Universitas Gadjah Mada, Bulaksumur BLS 21, Yogyakarta 55281, Indonesia.
e-mail (corresponding author): fakhrud@ugm.ac.id; ORCID: https://orcid.org/0000-0002-1540-6412.

[2] Department of Physics, Faculty of Mathematics and Natural Sciences, Universitas Gadjah Mada, Bulaksumur BLS 21, Yogyakarta 55281, Indonesia.
e-mail: hanif.nata.w@mail.ugm.ac.id; ORCID: https://orcid.org/0009-0001-1262-6815.

[*] Corresponding author.

§ Manuscript received: October 12, 2023; accepted: : July 17, 2024.
TWMS Journal of Applied and Engineering Mathematics, Vol.15, No.4;

where $\mathcal{L}$ is a linear operator and $N[u]$ is a nonlinear term which is a functional of u.

Apart from equation (1), the Swift-Hohenberg equation also has a complex form [3]:

$$\partial_t u = \epsilon u - (1 + \partial_x^2)^2 u - (1 + ib)u^3, \tag{3}$$

where b is the imaginary constant that plays a role in the dynamics that emerge.

For the real version of the equation, there are two possibilities for the solution u: it either decays or grows over time. Linear stability analysis was carried out to determine the behavior of the solution u. First, note that the ground state solution u_b is a steady state or has no spatial structure, namely $u_b = 0$. We then apply a small perturbation $u_p = u - u_b$ to check if u decays or grows. Let u_p evolve based on the equation [2]:

$$\partial_t u_p = \hat{N}(u_b + u_p) - \hat{N}(u_b), \tag{4}$$

where $\hat{N}$ is an operator that is a function of $u(x,t)$ and is defined from the right-hand term of equation (1):

$$\hat{N}(u) = \epsilon u - u - 2\partial_x^2 - \partial_x^4 u - u^3. \tag{5}$$

Equation (4) becomes:

$$\begin{aligned}\partial_t u_p \;\; = \;\; & (\epsilon - 1)(u_b + u_p) - \partial_x^4(u_b + u_p) - 2\partial_x^2(u_b + u_p) - (u_b + u_p)^3 \\ & -(\epsilon - 1)(u_b) - \partial_x^4(u_b) - 2\partial_x^2(u_b) - u_b^3.\end{aligned} \tag{6}$$

By linearizing equation (6) and using $u_b = 0$, the above equation becomes:

$$\partial_t u_p = (\epsilon - 1 - 2\partial_x^2 - \partial_x^4)u_p, \tag{7}$$

which can be rewritten as:

$$\partial_t u_p = \epsilon u_p - (1 + \partial_x^2)^2 u_p. \tag{8}$$

The above equation is analogous to the linear form of the Swift-Hohenberg equation (1) with the solution of an exponential form over time and space:

$$u_p = Ae^{(\sigma t + \alpha x)}, \tag{9}$$

where A is a constant and σ is the growth rate. Equation (9) is substituted into equation (8) to obtain the growth rate as a function of the control parameter ϵ and α:

$$\sigma = \epsilon - (\alpha^2 + 1)^2. \tag{10}$$

The constant α is determined by assuming that u_p has periodic boundary conditions with period L. Equation (9) will be periodic if:

$$e^{\alpha x} = e^{\alpha(x+L)}. \tag{11}$$

Equation (11) is fulfilled if $e^{\alpha L} = 1$, so $\alpha = \frac{i2\pi m}{L}$ where m is an integer. This can be simplified by setting $\alpha = iq$ and $q = \frac{2\pi m}{L}$, which is the wave number. The relationship between growth rate σ and wave number q is:

$$\sigma = \epsilon - (1 - q^2)^2. \tag{12}$$

The growth rate σ is maximum when the wave number q is equal to the critical wave number $q_c = 1$. When the control parameter is negative, the growth rate will also be negative, indicating system stability. When the control parameter is zero, the growth rate is zero at $q = q_c = 1$, indicating marginal stability of the system. When the control parameter is positive, the growth rate is positive for a certain range of wave numbers, leading to system instability. The plot of equation (12) for negative, zero, and positive ϵ is shown in Figure 1. For $\epsilon = 0.2$, there exists a small range of wave numbers around the critical wave number that contribute to the positive growth rate. An initial disturbance will grow, leading to instability. The existence of several unstable wave numbers will result in a solution in the form of a spatial periodic pattern (rolls) at the onset of the instability [4].

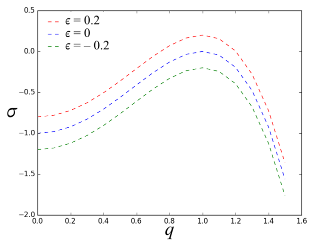

FIGURE 1. Dispersion relation of growth rate σ as a function of q obtained by linear stability analysis of the Swift-Hohenberg equation which fulfills equation (12). The unstable region $\sigma > 0$ occurs when the control parameter is positive [2].

In general, the transition from an ordered state to a chaotic state on various experimental systems and mathematical models occur through a scenario of intermittency or spatiotemporal intermittency [5, 6, 7]. The idea of the intermittency scenario was coined by Pomeau and Manneville (1980) when studying the Lorenz model [6]. They varied a control parameter r of the Lorenz model. When the control parameter is below the critical value $r_c = 166.06$ the dynamic shows periodic (regular) behavior. In the spatiotemporal intermittency (STI) scenario, the previously orderly or laminar state will become a chaotic state preceded by regular and chaotic states that appear simultaneously or coexist at certain control parameter values. On a time series graph, this is characterized by the presence of regular dynamics, such as periodic dynamics, which are then punctuated by an explosion (burst). This scenario towards chaos has been observed in the modified Swift-Hohenberg equation [7]

$$\partial_t u = \epsilon u - (\partial_{xx} + 1)^2 u - u\partial_x u, \tag{13}$$

that is equivalent to the damped Kuramoto-Sivashinsky equation [12, 13, 14]

$$\partial_t u + \eta u + \partial_{xx} u + \partial_{xxxx} u + 2u\partial_x u = 0. \tag{14}$$

The dynamics in the above equation is determined by two parameters, namely the system size D and the parameter η. For a fixed value of D, the control parameter is η. For the equation (14) an ordered state occurs at large η. By decreasing the value of η until the system becomes chaotic. Apart from modifications to the nonlinear term, there is research that adds a noise term, with which emergence bifurcation can be obtained [9, 10]. Research on original Swift-Hohenberg has mainly been carried out at low control parameter. This research will focus on the influence of using high control parameter and focus on the transition to chaotic dynamics.

2. Implementation of the Exponential Time Differencing (ETD) Scheme in the Swift–Hohenberg equation

To obtain the solution u, first we multiply it by the integrating factor $e^{-\pounds t}$ then we integrate between the limits t_n to t_{n+1}. The distance between two points in the domain t is $h = t_{n+1} - t_n$.

$$d_t e^{-\pounds t} u = e^{-\pounds t}\dot{u} - \pounds u e^{-\pounds t} \tag{15}$$

$$\int_{t_n}^{t_{n+1}} d\, e^{-\pounds t}u = \int_{t_n}^{t_{n+1}} e^{-\pounds t} H(u,t)\, dt. \tag{16}$$

By operating the integral of the left side of the equation we get

$$\left[ue^{-\pounds t}\right]_{t_n}^{t_{n+1}} = \int_{t_n}^{t_{n+1}} e^{-\pounds t} H(u,t)\, dt. \tag{17}$$

Where $t_n = 0$, $t_{n+1} = h$, and by introducing the new time variable τ in the integration as the time lag (substituting $H(u(t_n+\tau), t_n)$ to $H(u,t)$) we get

$$e^{-\pounds t_{n+1}} u_{t_{n+1}} - e^{-\pounds 0} u_{t_n} = \int_0^h e^{-\pounds \tau} H(u(t_n+\tau), t_n+\tau) d\tau. \tag{18}$$

Considering $e^{-\pounds 0} = 1$ and equating the above equation we get

$$u_{t_{n+1}} = \frac{u_{t_n} + \int_0^h e^{-\pounds \tau} H(u(t_n+\tau), t_n+\tau) d\tau}{e^{-\pounds t_{n+1}}} \tag{19}$$

$$u_{t_{n+1}} = u_{t_n} e^{\pounds h} + e^{\pounds h} \int_0^h e^{-\pounds \tau} H(u(t_n+\tau), t_n+\tau)\, d\tau \tag{20}$$

Equation (20) is a recurrence relation between $u_{t_{n+1}}$ and u_{t_n}. The order in the ETD scheme depends on the integrand $H(u(t_n+\tau), t_n+\tau)$ used in the calculation. ETD Scheme 1 is obtained by assuming the value of $H(u(t_n+\tau), t_n+\tau)$ in equation (20) is constant, denoted as H_n. Thus, we obtain the ETD 1 scheme

$$u_{n+1} = e^{\pounds h} u_n + e^{\pounds h} \int_0^h e^{-\pounds \tau} H_n\, d\tau \tag{21}$$

$$= e^{\pounds h} u_n + e^{\pounds h} \left[\frac{H_n e^{-\pounds h}}{-\pounds} - \left(\frac{H_n}{-\pounds}\right) e^{-\pounds 0}\right] = e^{\pounds h} u_n + \left[\frac{H_n e^{\pounds h}}{\pounds} - \frac{H_n}{\pounds}\right] \tag{22}$$

$$u_{n+1} = e^{\pounds h} u_n + \frac{H_n}{\pounds}\left(e^{\pounds h} - 1\right) \tag{23}$$

A higher order ETD scheme can be obtained by changing the integrand value which is not a constant along the interval $t_n \le t \le t_{n+1}$. Second order exponential time differencing (ETD2) scheme is obtained by assuming that the value $H(u(t_n+\tau), t_n+\tau)$ is

$$H = H_n + \frac{\tau}{h}\left(H_n - H_{n-1}\right). \tag{24}$$

So we get the ETD2 scheme

$$u_{n+1} = u_n e^{\pounds h} + \frac{H_n}{h\pounds^2}\left[(h\pounds+1)e^{\pounds h} - 2h\pounds - 1\right] + \frac{H_{n-1}}{h\pounds^2}(-e^{\pounds h} + h\pounds + 1). \tag{25}$$

To get a smaller relative error we combine the ETD2 with the fourth-order Runge-Kutta (RK4) method [8]. The ETDRK4 equation is as follows [15]:

$$\begin{aligned} u_{n+1} = u_n e^{ch} &+ H(u_n, t_n)[-4 - hc + e^{ch}(4 - 3hc + h^2c^2)] \\ &+ 2(H(a_n, t_n + h/2) + H(b_n, t_n + h/2))[2 + hc + e^{ch}(-2 + hc)] \\ &+ H(c_n, t_n + h)[-4 - 3hc - h^2c^2 + e^{ch}(4 - hc)]/h^2c^3 \end{aligned} \tag{26}$$

$$a_n = u_n e^{\frac{ch}{2}} + (e^{\frac{ch}{2}-1}) H(u_n, t_n)/c \tag{27}$$

$$b_n = u_n e^{\frac{ch}{2}} + (e^{\frac{ch}{2}-1}) H(a_n, t_n + h/2)/c \tag{28}$$

$$c_n = u_n e^{\frac{ch}{2}} + (e^{\frac{ch}{2}-1})(2H(b_n, t_n + h/2) - H(u_n, t_n))/c \tag{29}$$

3. Solving the Swift-Hohenberg Equation Using the ETDRK4 Scheme and Spectral Method

Equation (1) is a periodic equation whose solution will be calculated by approximating the solution u using the Fourier series. The approximate solution of u using the Fourier series is

$$u(x,t) = \sum_{m=1}^{N} \hat{u}_m e^{ik_m x}, \quad k_m = \frac{m\pi}{L} \tag{30}$$

$$\frac{\partial u(x,t)}{\partial t} = \sum_{m=1}^{N} \frac{\partial \hat{u}_m}{\partial t} e^{ik_m x} \tag{31}$$

$$\frac{\partial^2 u(x,t)}{\partial x^2} = -\sum_{m=1}^{N} k_m^2 \hat{u}_m e^{ik_m x} \tag{32}$$

$$\frac{\partial^4 u(x,t)}{\partial x^4} = \sum_{m=1}^{N} k_m^4 \hat{u}_m e^{ik_m x} \tag{33}$$

Substituting equations (30) to (33) into equation (1), we get

$$\partial_t \hat{u}_m = \left[(\epsilon - 1) + 2k_m^2 - k_m^4\right] \hat{u}_m - \left[\hat{u}_m^3 e^{(2k_m x_i)}\right] \tag{34}$$

$$\partial_t \hat{u}_m = \left[(\epsilon - 1) + 2k_m^2 - k_m^4\right] \hat{u}_m - \hat{\omega}_n \tag{35}$$

So we obtain ordinary differential equations in Fourier space. The equation (35) has the form of equation (2), so it can be solved using the ETDRK4 method with the value $\pounds = (\epsilon - 1 + 2k_m^2 - k_m^4)$ and $N(u,t) = \hat{\omega}_n = -\mathrm{FFT}(\mathrm{IFFT}(\hat{u})^3)$, where FFT is the fast Fourier transform and IFFT is the inverse fast Fourier transform.

Using ETDRK4, the nonlinear term in any functional form, including the cubic term, is treated in the wavenumber space. Essentially, we combine ETDRK4 and the spectral method to solve the Swift-Hohenberg equation by transforming the equation from physical space x to the wavenumber space k using the spectral method, and then solving the time t dependence of the resulting equation using ETDRK4. The details of the implementation of ETDRK4 combined with the spectral method on the Swift-Hohenberg equation have been previously described [16].

4. Results and discussions

4.1. **Real Swift-Hohenberg Equation.**

In this paper, the size of the system D and the number of truncations W in equations (1) remain constant across all simulations, with $(D,W) = (20\pi, 512)$, ensuring that the dynamics of equation (1) are solely influenced by the control parameter ϵ. To observe the dynamic behavior of the Swift-Hohenberg equation, a maximum time of $t_{\max} = 200000$ is utilized, with a time discretization $h = 0.05$. The control parameter values used are in the range $0 \leq \epsilon \leq 23.9$.

The dynamics of the Swift-Hohenberg equation are illustrated by the spatiotemporal plot in Figure 2. It demonstrates increasingly irregular and complex behavior as the control parameter is increased. Figure 2 (A) shows regular and constant dynamics for $\epsilon = 1.0$. When the control parameter is increased to $\epsilon = 22.0$, the dynamics remain regular and exhibit a spatially periodic solution. This is predictable considering the contribution of finite wavenumbers, as shown by the range of positive q in Figure 1.

As the control parameter is increased further, the dynamics transition into a periodic state. The spatiotemporal plot in Figure 2 (C) for $\epsilon = 22.4$ shows periodic changes

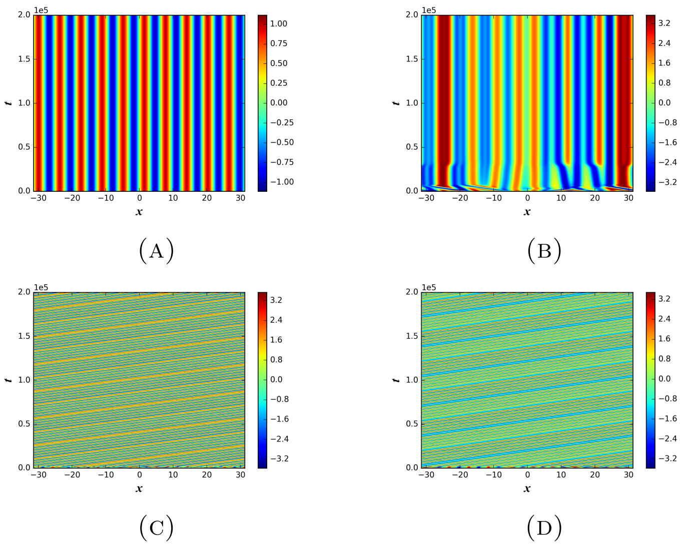

FIGURE 2. Spatiotemporal plot of solution u of the Swift-Hohenberg equation with spatial discretization $W = 512$, $\Delta x = 20\pi/512$, $t_{max} = 200000$ (A) for control parameter $\epsilon = 1$, (B) $\epsilon = 22.0$, (C) $\epsilon = 22.4$, and (D) $\epsilon = 22.6$. The colored legends on the right of each plots are indicating the value of u.

in solution values over time, forming a transverse strip pattern. The Swift-Hohenberg equation continues to exhibit periodic dynamics until the control parameter reaches $\epsilon = 22.6$.

More complex dynamics emerge with further increases in the control parameter. Figure 3 shows the spatiotemporal dynamics for the following control parameter values: (a) $\epsilon = 22.7$, (b) $\epsilon = 22.8$, (c) $\epsilon = 23.0$, and (d) $\epsilon = 23.6$. It can be observed that the dynamics become irregular for control parameter values $\epsilon \geq 23.0$.

The dynamics of the Swift-Hohenberg equation for a fixed control parameter value can be described through a time series graph at one point in the variable space. Figure 4 illustrates the dynamics produced by the Swift-Hohenberg equation. The time series graph shows that for a control parameter of 22, the dynamics are regular and constant. Figures 4 (b) and (c) show the time series graph for control parameters 22.4 and 22.7, respectively, exhibiting regular dynamics that appear periodic and quasiperiodic, in harmony with the spatiotemporal graph. This is because the control parameter has reached the critical value, resulting in a Hopf bifurcation that produces periodic dynamics. As the control parameter increases further, the time series graph becomes irregular and displays chaotic dynamics, as shown in Figure 4 (d) with $\epsilon = 23.6$. The transition from regular to chaotic dynamics in the Swift-Hohenberg equation at high control parameters occurs through a scenario of intermittency or spatiotemporal intermittency, similar to that in other systems, as reported in previous research [5, 6, 7].

To further characterize the dynamics of the Swift-Hohenberg equation, a power spectrum analysis is performed. The temporal power spectrum function of a discrete-time series $u(t_q)$ is defined as [11]

$$S_j \equiv S_{\omega_j} = |\hat{u}_x(\omega_j)|^2 \tag{36}$$

where $\hat{u}_x(\omega_j)$ is a temporal discrete Fourier transform, which is the amplitude of each harmonic that forms the time series data. The temporal discrete Fourier transform is

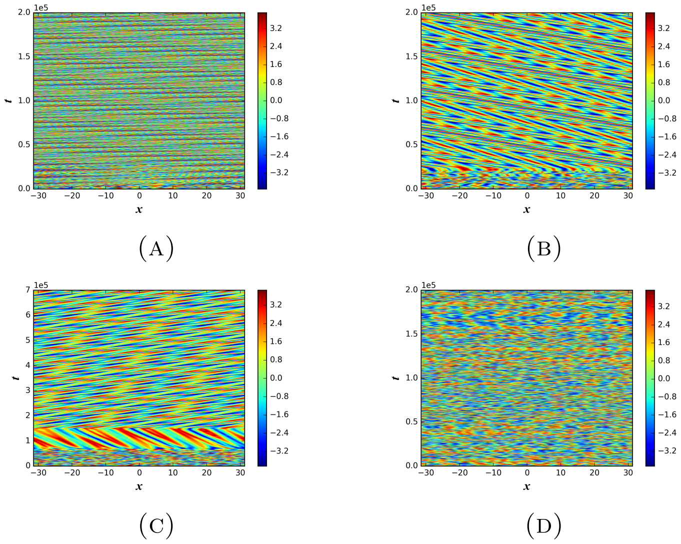

FIGURE 3. Spatiotemporal plot of the solution of the Swift-Hohenberg equation with spatial discretization $W = 512$, $\Delta x = 20\pi/512$, $t_{max} = 200000$ (A) for control parameter $\epsilon = 22.7$, (B) $\epsilon = 22.8$, (C) $\epsilon = 23.0$, and (D) $\epsilon = 23.6$.

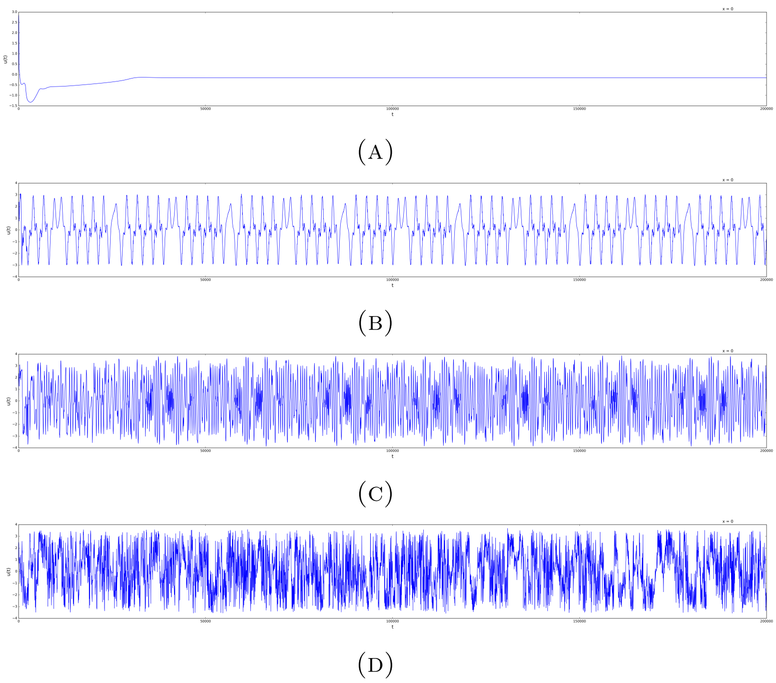

FIGURE 4. Fluctuation of u obtained by solving the Swift-Hohenberg equation with spatial discretization $W = 512$, $\Delta x = 20\pi/512$, $t_{max} = 200000$ (A) for control parameter $\epsilon = 22.0$, (B) $\epsilon = 22.4$, (C) $\epsilon = 22.7$, and (D) $\epsilon = 23.6$.

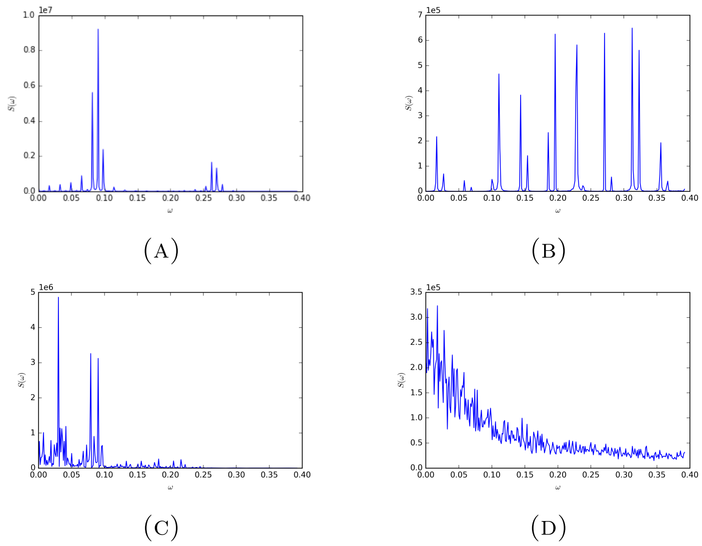

FIGURE 5. Power spectrum graphs of Swift-Hohenberg equation solutions for (A) $\epsilon = 22.4$, (B) $\epsilon = 22.7$, (C) $\epsilon = 22.8$, and (D) $\epsilon = 23.6$.

defined as

$$\hat{u}_x(\omega_j) = \frac{1}{Q}\sum_{q=0}^{Q-1} u_x(t_q)e^{-i\omega_j t_q} \tag{37}$$

where $\omega_j = \frac{2\pi j}{Q}$ with $j = 0, 1, .., Q-1$ and $t_q = \frac{qT}{Q}$ with $q = 0, 1, ..., Q-1$.

Figure 5(A) illustrates the results of the power spectrum analysis of the Swift-Hohenberg equation with a control parameter of $\epsilon = 22.4$. In the power spectrum graph, there are some peaks, indicating that the dynamics generated by the Swift-Hohenberg equation contain some frequencies. The spatiotemporal diagram with control parameter values below 22.4 also exhibits similar behavior, as shown in Figure 2(A) and (B). Similarly, the time series graph depicts consistent dynamics, as shown in Figure 4(A).

Within a certain range of the control parameter, the Swift-Hohenberg equation generates periodic and quasiperiodic dynamics. Periodic dynamics are characterized by the presence of a fundamental frequency along with its harmonic frequencies in the power spectrum analysis. The existence of fundamental frequencies can be seen in the peaks ($q < 0.05$) of the power spectrum of the pre-chaotic state (see Figure 5(B)) which persist in the chaotic state as suggested by Ruelle-Takens and Newhouse's route to chaos theory [17]. The transition to periodic dynamics occurs when the control parameter reaches a critical value, leading to Hopf bifurcation and the emergence of periodic dynamics. Periodic dynamics occur within the control parameter range $22.4 \leq \epsilon < 22.7$. When the control parameter is increased to $\epsilon = 22.4$, the power spectrum graph in Figure 5(A) displays the presence of one fundamental frequency and its harmonic frequencies. In Figure 5(B), with the control parameter set to $\epsilon = 22.7$, two fundamental frequencies appear, indicating quasiperiodic dynamics. This suggests that a control parameter value of 22.7 is a critical point where the second Hopf bifurcation occurs, resulting in quasiperiodic dynamics. Quasiperiodic dynamics continue in the Swift-Hohenberg equation for control parameter in the range of 22.8 to 23.0, revealing some frequencies in the power spectrum graph.

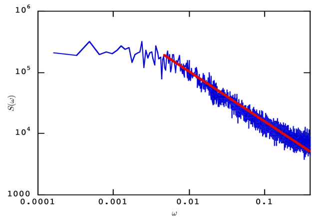

(A)

FIGURE 6. Power spectrum S_j of the solution of the Swift-Hohenberg equation for $\epsilon = 23.6$ in the log-log plot. The red line follows $S(\omega) \propto \omega^{-0.81}$.

Quasiperiodic dynamics eventually evolve into chaotic dynamics, characterized by a broadband spectrum in the power spectrum analysis. By varying the control parameter from $\epsilon = 0$ up to $\epsilon = 25$, we observed that chaotic dynamics manifest within the control parameter range of $23.1 \leq \epsilon \leq 23.9$. The power spectrum graph of chaotic dynamics exhibits a broadband spectrum, as illustrated in Figure 5 (D). For instance, when the control parameter is set to $\epsilon = 23.6$, the presence of a broadband spectrum indicates chaotic dynamics. To verify the dynamics at $\epsilon = 23.6$, we calculated the Lyapunov exponent [18] (the Python program is available in [19]). The chaotic dynamics at $\epsilon = 23.6$ are confirmed by the positive Lyapunov exponent ($\lambda > 0$). In the chaotic state, the power spectrum shows a power-law behavior of $S(\omega) \propto \omega^{-0.81}$, as shown in Figure (6). Thus, we demonstrate that the power spectrum behavior of chaotic dynamics in the Swift-Hohenberg equation is similar to that observed in turbulent flow.

4.2. **The Complex Swift-Hohenberg Equation.** As mentioned earlier, the Swift-Hohenberg equation with complex terms is expressed as follows [3]:

$$\partial_t u(x,t) = \epsilon u(x,t) - (1 + \partial_x^2)^2 u(x,t) - (1 + ib) u(x,t)^3. \tag{38}$$

In this study, the parameter b is varied while ϵ is kept constant at $\epsilon = 1$. The system size for the simulation is $D = 300$ with a spatial discretization of $W = 1024$. The integration is carried out using the ETDRK4 method over a period of $t_{max} = 200000$ with a time discretization of $\delta t = 0.05$. The resulting dynamics are observed as the control parameter b is varied in the range $-8 \leq b \leq 0$. The most straightforward solution occurs when $b = 0$ because the Swift-Hohenberg equation returns to its real form, as depicted in Figure 7 (A).

For certain values of the parameter b, the complex Swift-Hohenberg equation exhibits regular dynamics. When $b = -1$, the spatiotemporal plot remains regular. However, as b is changed to -4, a small chaotic region emerges alongside predominantly ordered dynamics. Further increasing the absolute value of b to -5 results in a larger chaotic region with diminishing regular dynamics. Intermittent behavior becomes evident in the spatial coordinate, particularly at $b = -5.5$, where chaotic areas dominate, and regular areas dwindle. Ultimately, as $b \leq -7$, the complex Swift-Hohenberg system transitions to spatiotemporal chaos, as depicted in Figure 7, where regular dynamics become challenging to discern, and chaos prevails.

The temporal dynamics of a point in space, specifically at $x = 0$, from the complex Swift-Hohenberg equation with parameter values around $b \approx -5.5$, are illustrated in Figure 8. At a control parameter value of $b = -5$, the time series graph at $x = 0$ exhibits regular dynamics. As the parameter b increases, an irregular time series region emerges, as seen in Figures 8 (B), (C), and (D). Within the b parameter range, regular dynamics coexist

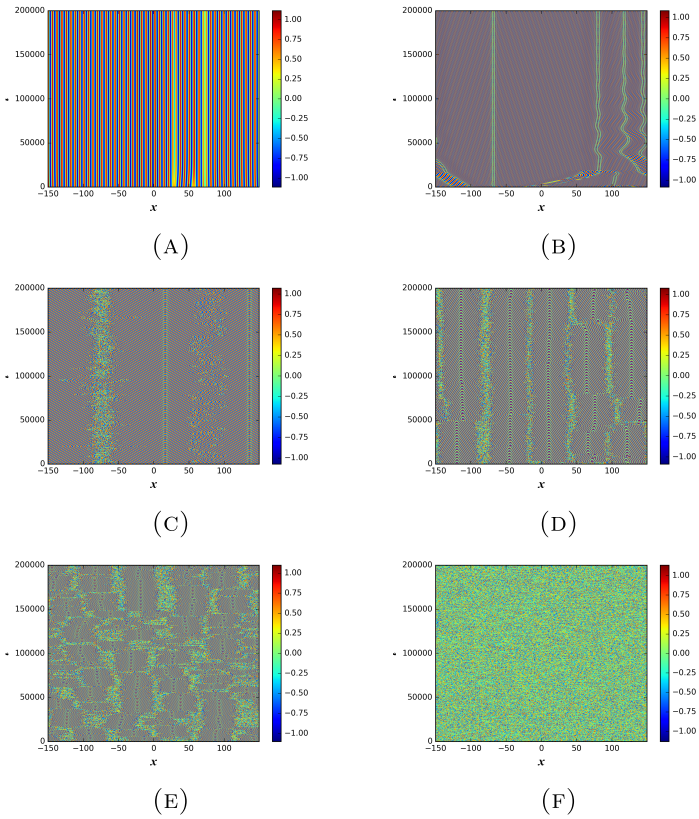

Figure 7. Spatiotemporal plot of the solution of equation (38) with spatial discretization $W = 512$, $\Delta x = 20\pi/512$, $t_{max} = 200000$, control parameter $\epsilon = 1$, and for $b = 0, -1, -4, -5, -5.5, -8$ from (A) to (F), respectively.

with irregular or chaotic dynamics. With further increases in the parameter b, the time series graph reveals irregular or chaotic dynamics, as evidenced at $b = -8$.

The spatiotemporal plot in Figure 7 demonstrates spatial intermittency when $b = -4$, and as b decreases, intermittency becomes more pronounced. Power spectrum analysis within the $-8 \leq b \leq -6$ parameter range unequivocally confirms the presence of chaotic spatiotemporal dynamics. This is evident from the broadband noise exhibited on the power spectrum graph, a hallmark of chaotic behavior. The Lyapunov exponent value of the solution of the Swift-Hohenberg equation at complex parameter $-8 \leq b \leq -6$ is positive.

5. Conclusions

Numerical solutions of the original Swift-Hohenberg equation have been obtained at high control parameter values. Chaotic dynamics are observed when the control parameter is sufficiently high, specifically at $\epsilon = 23.6$, as evidenced by a spectrum with significant background noise. Additionally, a quantitative analysis of the dynamics using Lyapunov exponents consistently shows positive values, indicating the chaotic behavior of the field u.

Furthermore, we have investigated the Swift-Hohenberg equation with complex terms, primarily at a relatively low control parameter value of $\epsilon = 1.0$, allowing us to focus on variations in the complex constant. The results indicate that for specific ranges of the h 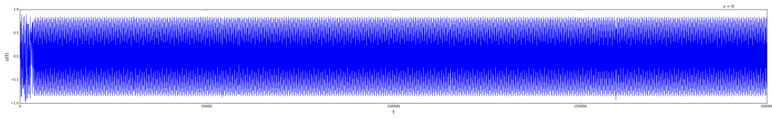

(A)

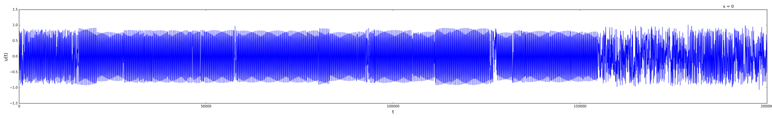

(B)

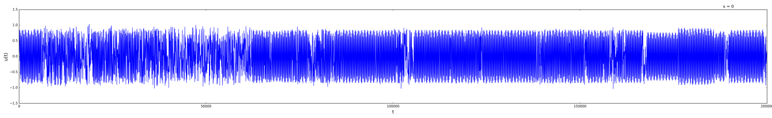

(C)

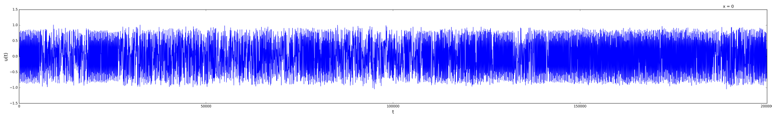

(D)

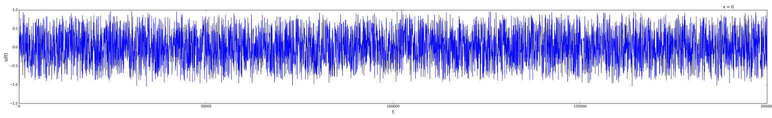

(E)

FIGURE 8. Fluctuation of u obtained by solving equation (38) with $b = -5.0, -5.3, -5.4, -5.5, -8$ in (A)-(E), respectively.

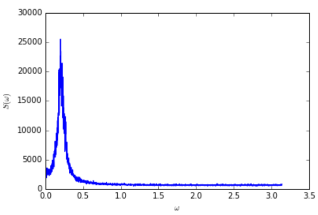

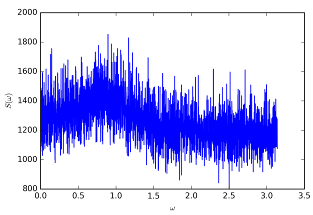

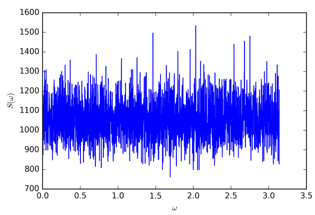

h

(A) (B) (C)

FIGURE 9. Power spectrum of the solution of equation (38) with $b = -6$ (A), $b = -7$ (B), and $b = -8$ (C).

complex constant, chaotic dynamics also emerge. Consequently, our study elucidates the transition to chaos in both the real and complex variants of the Swift-Hohenberg equation.

Acknowledgments. This work was partially supported by The Directorate General of Higher Education of Indonesia Contract Contract Number PUPT 119/LPPM/2015 and Number PDUPT 74/LPPM/2018.

References

[1] Swift J., Hohenberg, P. C., (1977). Hydrodynamic fluctuations at the convective instability, Phys. Rev. A., 15 (1), pp. 319–328

[2] Cross, M. C. dan Greenside, H., (2009), Pattern Formation and Dynamics in Nonequilibrium Systems, Cambridge University Press, New York.

[3] Gelens, L., Knobloch, E., (2011), Travelling Waves and Defects in Swift-Hohenberg Equation, Physical Review E 84.

[4] Cross, M. C. dan Hohenberg, P. C., (1993), Pattern Formation Outside Equilibrium, Rev. Mod. Phys. **65**: 851-1112

[5] Kaneko, K., (1985), Spatiotemporal Intermittency in Coupled Map Lattice, Progress of Theoretical Physics 75 (5): 1033 - 1044

[6] Pomeau, Y., Manneville, P., (1980), Intermittent Transition to Turbulence in Dissipative Dynamical Systems, Communication in Mathematical Physics 74: 189 - 197

[7] Chate, H., Manneville, P., (1987), Transition to Turbulence via Spatiotemporal Intermittency, Physical Review Letters 58 (2): 112 - 115

[8] Burden, R. L., dan Faires, J. D., (2011), Numerical Analysis Ninth Edition, Brooks/Cole Cengage Learning, Boston.

[9] Elphick, C., Tirapegui, E., Brachet, M. E., Coullet, P., and Iooss, G. (1987). A simple global characterization for normal forms of singular vector fields. Physica D: Nonlinear Phenomena, 29(1–2), 95–127.

[10] Agez, G., Clerc, M. G., Louvergneaux, E., and Rojas, R. G. (2013). Bifurcations of emerging patterns in the presence of additive noise. Physical Review E - Statistical, Nonlinear, and Soft Matter Physics, 87(4).

[11] Argyris, J., Faust, G., Haase, M., Friedrich, R., (2015), An Exploration of Dynamical System and Chaps, Springer-Verlag, Berlin.

[12] Kuramoto, Y., (1978), Progress of Theoretical Physics Supplement, 64, 346–367

[13] Sivashinky, G.I., (1980), SIAM Journal on Applied Mathematics, 39 (1) 67-82

[14] Sivashinky, G. I., Acta Astronautica, (1977), 4(11), 1177-1206

[15] Cox, S.M., Matthews, P. C., (2002), Exponential Time Differencing for Stiff Systems, Journal of Computational Physics., 176, pp. 430-455.

[16] Wijaya, H. N., 2018, Numerical Simulation of The Sift-Hohenberg Equation Using Exponential Time Differencing Runge Kutta 4 and Pseudospectral Methods, Bachelor Thesis, (Unpublished).

[17] Schuster, H. G. and Just, W., (2005). Deterministic Chaos: An Introduction, WILEY-VCH Verlag GmbH & Co. KGaA, 129-130

[18] Rosenstein, M. T., Collins, J. J., and De Luca, C. J. (1993). A practical method for calculating largest Lyapunov exponents from small data sets. Physica D, 65(1–2), 117–134.

[19] https://cschoel.github.io/nolds/nolds.html

Fahrudin Nugroho received B.Sc. and M.Sc. from Gadjah Mada University, Yogyakarta, Indonesia, in 2004 and 2007, respectively. He received his Ph.D. from Kyushu University, Japan in 2012. He is a lecturer at Gadjah Mada University. His main research interests are chaos and nonlinear dynamics.

Hanif Nata Wijaya graduated from Gadjah Mada University, Yogyakarta, Indonesia, in 2018. His research topic was dynamics of nonlinear equation. Additionally, he pursued professional teacher education organized by the Ministry of Education, Culture, Research, and Technology and graduated in 2023. He is currently becoming a teacher at a public high school in Temanggung, Central Java, Indonesia.